The International Journal of Biochemistry & Cell Biology 79 (2016) 437–442

Contents lists available at ScienceDirect

The International Journal of Biochemistry & Cell Biology

journal homepage: www.elsevier.com/locate/biocel

Review article

Recent advances in the structural biology of the 26S proteasome

Marc Wehmer, Eri Sakata*

Department of Molecular Structural Biology, Max Planck institute of Biochemistry, 82152, Martinsried, Germany

ARTICLE INFO

Article history:
Received 28 June 2016
Received in revised form 2 August 2016
Accepted 3 August 2016
Available online 4 August 2016

Keywords:
26S proteasome
Cryoelectron microscopy
Single particle analysis
Structural biology
AAA+ ATPase

ABSTRACT

There is growing appreciation for the fundamental role of structural dynamics in the function of macromolecules. In particular, the 26S proteasome, responsible for selective protein degradation in an ATP dependent manner, exhibits dynamic conformational changes that enable substrate processing. Recent cryo-electron microscopy (cryo-EM) work has revealed the conformational dynamics of the 26S proteasome and established the function of the different conformational states. Technological advances such as direct electron detectors and image processing algorithms allowed resolving the structure of the proteasome at atomic resolution. Here we will review those studies and discuss their contribution to our understanding of proteasome function.

Contents

1. Introduction

The ubiquitin-proteasome system (UPS) is involved in many cellular processes through the maintenance of proteostasis, and the malfunction of this system leads to a broad array of diseases, including cancer, viral infection and neurodegeneration (Labbadia and Morimoto, 2015; Petroski, 2008; Schwartz and Ciechanover, 2009). The UPS regulates protein levels in eukaryotic cells by hydrolyzing specific targeted proteins into small peptides (Finley, 2009). Selection of degradation targets is made by ubiquitin conjugation, utilizing the small protein ubiquitin as destruction marker (Hershko and Ciechanover, 1998). The length and type of linkage of the ubiquitin chain influence the recognition and degradation by the proteasome, and generally chains of at least four K48-linked ubiquitin moieties are necessary for delivery to the proteasome (Haglund and Dikic, 2005; Thrower et al., 2000).

The 26S proteasome is a cylinder-shaped particle that consists of 33 canonical subunits arranged into two complexes: the 20S core particle (CP) and one or two 19S regulatory particle (RP) at each end of the CP (Voges et al., 1999). Proteolytic cleavage of substrates takes place in the central CP cavity, which harbors the active sites. The 20S CP is made up by duplicating seven α subunits and seven β subunits, which form four axially stacked heteroheptameric rings (Groll et al., 1997). The 19S RP is a ~900 kDa protein complex containing at least 19 subunits and biochemically further divided into the base and the lid subcomplexes (Glickman et al., 1998). The base consists of six AAA+ ATPases (Rpt1–6) forming a hexameric ring, two scaffold proteins (Rpn1 and Rpn2) together with two ubiquitin receptors (Rpn10 and Rpn13). In addition to these intrinsic ubiquitin receptors, Rpn1 and Sem1 were found to recognize ubiquitinated substrates (Paraskevopoulos et al., 2014; Shi et al., 2016). The lid consists of six proteasome-COP9/signalosome-eIF3 (PCI)-containing subunits (Rpn3, 5, 6, 7, 9 and 12), two Mpr1–Pad1–N-terminal (MPN) subunits (Rpn8 and Rpn11) and the small adhesive protein Sem1. Among the lid subunits, only

* Corresponding author.
E-mail address: sakata@biochem.mpg.de (E. Sakata).

http://dx.doi.org/10.1016/j.biocel.2016.08.008

Rpn11 harbors catalytic activity as a Zn^{2+} dependent deubiquitylating enzyme (DUB) (Verma et al., 2002; Yao and Cohen, 2002). To penetrate the narrow axial channel from the ATPase to the 20S CP, substrates need to be unfolded and deubiquitylated prior to translocation. Thus, the proteasome cleaves polypeptides via a multistep sequential process that involves substrate recognition, unfolding, translocation and deubiquitylation (Finley, 2009). The 26S proteasome also often harbors several proteasome interacting proteins (PIPs) that interact transiently, including deubiquitylating enzymes, ubiquitin receptors, ubiquitin ligases as well as chaperones required for assembly (Finley, 2009).

The first insights into 26S proteasome structure were provided by negative stain electron micrographs in the early 90s, showing that one or two electron densities were attached to the ends of the 20S CP (Peters et al., 1993). Later, the structural determination of the 26S proteasome by cryo-EM single particle analysis was hindered by the instability of the holocomplex and its compositional and conformational heterogeneity. In addition, the 26S proteasome often exhibited unequal orientations in the ice because of its rather elongated structure, thereby preventing high resolution single particle 3D reconstruction. However, several intriguing findings were made by early structural studies with medium resolution. For example, it was clear that the central axis of the ATPase modules were not aligned to the one of the CP in drosophila and yeast proteasomes; both ATP modules were shifted by ~20 Å and respectively tilted by ~10° or ~4° with respect to the axis of the CP (Bohn et al., 2010; Nickell et al., 2009). Based on protein–protein interaction data and conformational requirements of cis prolines of Rpt2, Rpt3 and Rpt6, the arrangement of the Rpt subunits was computationally analyzed and proposed in the order of Rpt1/Rpt2/Rpt6/Rpt3/Rpt4/Rpt5 (Forster et al., 2009), which was later confirmed experimentally (Bohn et al., 2010; Tomko et al., 2010). Recently, a series of higher resolution cryo-EM studies allowed to assign each electron density to the proteasome subunits and thereby revealed a detailed view of the mechanisms by which the 26S proteasome accurately process polypeptides for degradation. In this review, we will provide an overview of those structural studies on the 26S proteasome.

2. Structural dynamics of the 26S proteasome

The assignment of all subunits to the electron density of the 26S complex was done by a combination of mutagenesis, protein-labeling, homology modeling, X-ray crystallography, crosslinking-MS and computational analysis (Fig. 1) (Beck et al., 2012; da Fonseca et al., 2012; He et al., 2012; Lander et al., 2012; Lasker et al., 2012; Pathare et al., 2012; Sakata et al., 2012).

All approaches resulted in essentially the same subunit localization. Although the base complex was hypothesized to serve as a basal scaffold of the RP at the interface to the CP, and the lid to cover the central channel of the ATPase ring, the actual localization of 19S subunits contradicted this notion. The base subunits, Rpn2, 10 and 13 are distally located and not associated with the 20S CP. Both ubiquitin receptors (Rpn10 and 13) are positioned in the apical part of the RP near the periphery, where they are well suited as receivers of ubiquitylated substrates (Sakata et al., 2012). Interestingly, the architecture of the lid complex is similar to that of functionally diverse complexes such as the COP9 signalosome and eIF3 (Lingaraju et al., 2014; Querol-Audi et al., 2013). The PCI subunits, Rpn3, 5, 6, 7, 9 and 12 assemble into a horseshoe-like configuration through their conserved PCI domains to harbor the Rpn8/11 heterodimer, connecting the base and 20S at the periphery. The assignment of all these canonical subunits was completed in the structure of the yeast 26S proteasome at 7.4 Å resolution (Beck et al., 2012). That structure resolved a density of a helix bundle composed of the C-terminal helices of the lid subunits located above the 'mouth' of the ATPases. This bundle was later found to self-assemble to scaffold the formation of the entire lid complex (Estrin et al., 2013; Tomko and Hochstrasser, 2011; Tomko et al., 2015).

Subsequent EM studies in the presence of ATPγS or a polyubiquitylated model substrate led to the discovery of a different conformational state (Matyskiela et al., 2013; Sledz et al., 2013). In addition, application of a novel image-classification strategy to a very large dataset of more than 3 million individual particles led to the deconvolution of further coexisting conformational states, revealing three major conformations (s1, s2, s3) (Unverdorben et al., 2014). The s1 state is the major conformation in ATP-containing buffer, while the s3 conformation is predominantly found in the presence of ATPγS or a polyubiquitylated model substrate. The central channel of the ATPase ring and the CP are not axially aligned in the s1 state, whereas they are aligned in the s3 state as a result of the dynamic rearrangement of the ATPase ring and lid subcomplex, presumably allowing substrates to access the catalytic chamber (Matyskiela et al., 2013; Sledz et al., 2013; Unverdorben et al., 2014). In the s3 state, the Rpn8/11 heterodimer is shifted by 25 Å, positioning the DUB catalytic site of Rpn11 along the central axis of the ATPase ring (Fig. 2, middle column). Rpn6 hinges Rpt6 of the RP and α2 of the CP in the s1 state. The N-terminal α-solenoid domain of Rpn6 undergoes a conformational rearrangement by rotating around its long axis, leading to its dissociation from the ATPase ring and the CP in the s3 state (Fig. 2, small inset). Interestingly, the relative configurations of the ubiquitin receptors are also altered by the conformational changes from s1 to s3. Rpn10 is in closer proximity to the mouth of the ATPase ring in s3, while Rpn1 rotates anticlockwise to make room for PIPs or the substrate binding. The overall s2 structure is more similar to the s3 than the s1 including the coaxial alignment of Rpn11 with the ATPase ring. The AAA module is slightly rotated and shifted, resulting in more coaxial alignment with the CP but less than in the s3 state. Based on this structural information, a functional model was proposed: A ground state (s1) where the proteasome is ready to accept substrates, an intermediate state (s2) where the substrate becomes positioned above the mouth of the ATPase module and a commitment state (s3) where substrate is translocated into the core complex to be degraded (Unverdorben et al., 2014).

The conformational variability of the proteasome was also observed *in situ*. A cryo-electron tomography study employing a direct electron detector and a new phase plate succeeded to localize individual 26S proteasomes within intact hippocampal neurons and assessed the activity status of each complex: only 20% of analyzed 26S proteasomes were in the s3 state in neuronal processes (Asano et al., 2015). Presumably, the activity of the proteasome is spatially and temporally regulated and the population of the active proteasomes might be affected by cellular conditions (e.g. cellular stress, cell cycle, aging) and sub-cellular localization. Interestingly, the *in situ* holocomplex in the s3 state showed an extra density in the proximity of the mouth of the ATPase module, indicating dynamic protein interactions in the active state. Thus, the combination of *in vitro* and *in vivo* studies revealed the fundamental role of structural dynamics in proteasome function.

3. Mechanical insights into the proteasome

The conformational changes in the ATPase module play a key role in substrate unfolding and translocation. The ATPase motor is suggested to translocate the polypeptide by a paddling movement of the aromatic hydrophobic (Ar-Φ) pore-1 loop that protrudes into the central channel (Matyskiela et al., 2013; Nyquist and Martin, 2013; Schweitzer et al., 2016; Sledz et al., 2013; Unverdorben et al.,

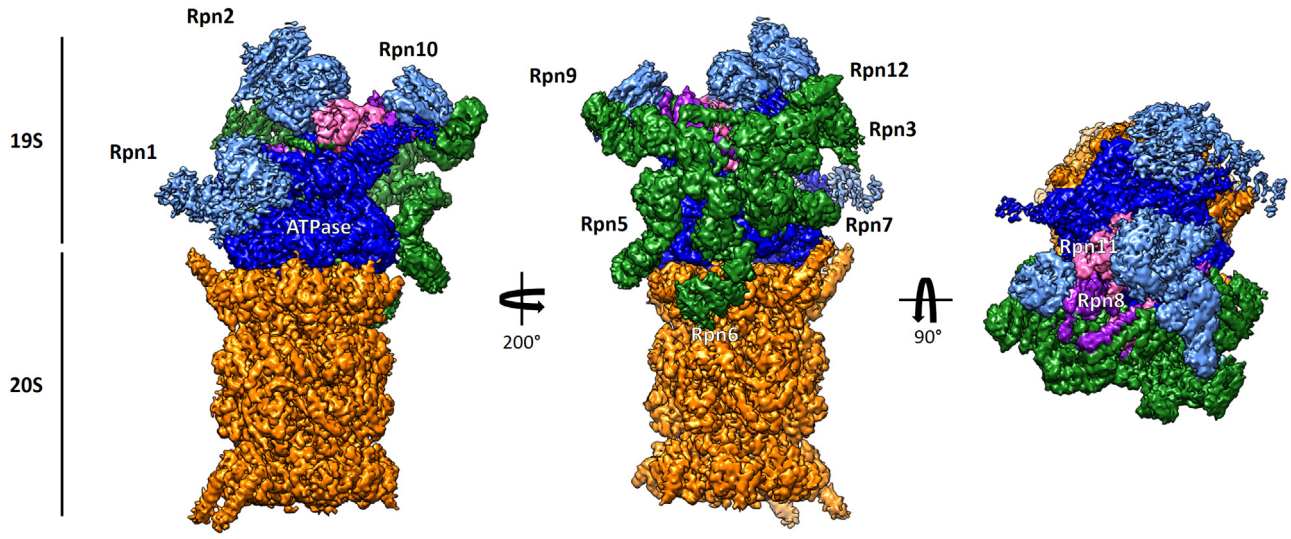

Fig. 1. 4 Å structure of the human 26S proteasome (EMDB: 4002, PDB: 5l4k, 5l4g). The EM density maps are colored: 20S core particle (orange), AAA+-ATPase (blue), Rpn1,2,10 (light blue), Rpn3,5,6,7,9,12 (green), Rpn8 (purple), Rpn11 (pink).

2014). The pore-1 loops contain conserved aromatic hydrophobic residues and interact with hydrophobic patches of extended polypeptides (Koga et al., 2009; Martin et al., 2008). The ATPase subunits are formed by a C-terminal AAA+ ATPase domain and an N-terminal OB ring connecting the coiled-coil motifs at their N-termini (Fig. 3A). Each ATPase domain is further divided into a large and a small ATPase domain, connected by a hinge region. The interface between the large and the small domains of the counterclockwise adjacent subunit is preserved in a 'rigid-body' fashion, in which conserved nucleotide-binding pockets are positioned in a specific configuration (Fig. 3B). Homologous to the well-characterized bacterial homolog ClpX, the nucleotide-binding pocket contains five defining conserved motifs, Walker A and Walker B, sensor 1, sensor 2 and arginine finger, at the interface between the large domain and the small domain (Erzberger and Berger, 2006; Nyquist and Martin, 2013; Wendler et al., 2012). The proteasome has double 'trans' Arg residues in the arginine finger, which project out to the small domain of the adjacent subunit to harbor a nucleotide in a 'trans' manner (Kim et al., 2015). In the s1 structure, which is characterized by off-axis positioning of the ATPase ring with respect to the CP, the large domain of Rpt3 and the small domain of Rpt6 break the rigid body configuration and form an 'open' conformation, which resembles the structure of the ADP-bound form of the proteasome-activating nucleotidase (PAN). The double Arg residues in the arginine finger of Rpt3 are not deployed towards Rpt6 (Fig. 3C). In contrast, the rest of the ATPase subunits form a 'closed' rigid-body structure to arrange the double Arg residues in the 'trans' position (discussed below). The 'open' structure is created by an arrangement of the ATPase subunits in which the Rpt subunits assemble as an asymmetrical 'split washer' in the hexamer (Fig. 3B) (Lander et al., 2012). A consequence of this organization is that the pore-1 loops arrange in a spiral staircase (Nyquist and Martin, 2013).

A dynamic structural change induces the interface between the large domain of Rpt1 and the small domain of Rpt5 to adopt the 'open' conformation (Matyskiela et al., 2013; Sledz et al., 2013). The 'open' structure between Rpt1 and 5 is caused by rearrangement of the spiral staircase in which each the rigid bodies are tilted to different extents (Lander et al., 2012; Matyskiela et al., 2013). The configuration of the ATPase ring in the s1 state is in a steep staircase arrangement, whereas it forms a more planar staircase arrangement in the s3 . Interestingly, those spiral staircase arrangements were observed in several DNA helicases, which propel DNA upon ATP hydrolysis (Enemark and Joshua-Tor, 2006; Thomsen and Berger, 2009). Followed by the rearrangement of the staircase upon ATP hydrolysis, the six pore-1 loops are also rearranged, which is translated to the mechanical force of translocation of the polypeptide. Compared to ClpX or PAN, however, the dynamics of the Rpt ATPase ring, which include the paddling movement of the pore-1 loops, may be suppressed because of the interaction with surrounding subunits. Further structural and biophysical studies will be required to better understand the mechanisms by which the ATPases transforms the energy of ATP hydrolysis into mechanical force and by which they grip the translocating polypeptide.

4. High resolution structure of the 26S proteasome

All hitherto published structures of the 26S proteasome were based on data acquired by conventional CCD cameras. With the advent of direct electron detectors it is now possible to attain higher resolution with fewer individual particles (the 'resolution revolution') (Kuhlbrandt, 2014; Nogales and Scheres, 2015). Not only the detective quantum efficiency of direct detectors is much improved, but their fast readout allows data recording in movie mode to compensate for beam-induced motions, a major resolution-limiting factor (Bai et al., 2013; Li et al., 2013).

The high resolution structure of the isolated lid complex revealed the activation mechanism of the DUB Rpn11 (Dambacher et al., 2016). The lid complex exhibits a large conformational change upon integration into the 26S holocomplex (Fig. 2). The PCI horseshoe in the isolated lid complex is in an open conformation and the spiral pitch is more tilted compared to the integrated complex. The most prominent rearrangement is the rotation of the MPN dimer. As the other MPN DUBs, Rpn11 contains two essential insertions, Ins-1 and Ins-2 (Lingaraju et al., 2014; Sato et al., 2008). The ins-1 loop of Rpn11 is locked in the inactive 'closed' conformation via an interaction with the adjacent subunit Rpn5 in the isolated lid complex. The DUB activity of Rpn11 is significantly inhibited in the isolated lid, whereas it is recovered in the holocomplex by a conformational change of the Ins-1 loop upon ubiquitin binding (Verma et al., 2002; Worden et al., 2014; Yao and Cohen, 2002). Thus, the DUB activity of Rpn11 prior to the integration into the holocomplex is regulated by Rpn5, presumably to prevent decoupling of deubiquitylation from degradation in cells. The ins-2 loop of Rpn11, which is used for the recognition of Lys63 ubiquitin chains

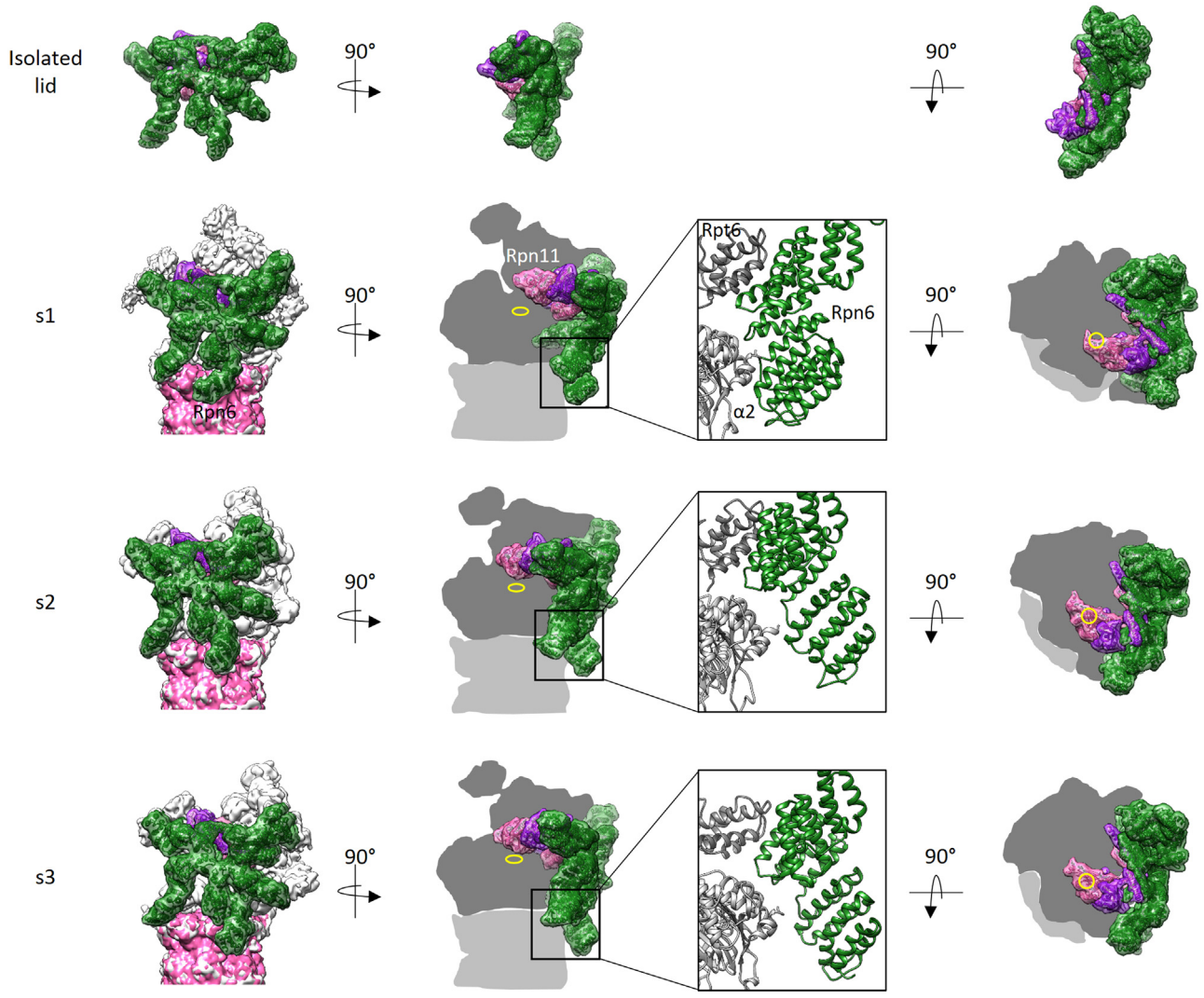

Fig. 2. Comparison of the lid configuration of the 26S proteasome in different states. The atomic models (pdb: 3jck, 4cr2, 4cr3, 4cr4) of the lid subunits (Rpn3,5,6,7,9,12) are shown in green, Rpn8 purple and Rpn11 in pink. The corresponding EM densities were simulated with a resolution of 10 Å using UCSF Chimera. In case of the 26S proteasome, the densities of the core particle (light grey) and base (dark gray) are depicted as shadows in column two and three, arising from the corresponding EM densities shown in column one (EMDB: 2594,2595,2596). The position of the substrate entry channel of the AAA-ATPase is shown as a yellow circle. The first row shows the isolated lid, the second row the s1 state, the third row the s2 state and the last row the s3 state. The interactions of Rpn6 (green) with α2 (light grey) and Rpt6 (dark grey) in the three different states of the proteasome are highlighted in the black boxes.

in the associated molecule with the SH3 domain of STAM (AMSH) DUB, is rather used for interaction with Rpn2 in the RP (Sato et al., 2008). In addition, a lid assembly study revealed that the incorporation of Rpn12 triggers an allosteric conformational change of the N-terminal solenoid domain of Rpn6, leading to the incorporation of the ATPase subunits to form the lid holocomplex (Tomko et al., 2015). EM analysis showed that the integration of the C-terminal helix of Rpn12, which forms a helix bundle with other lid subunits, induces an allosteric conformational change to extend Rpn6 outwards. The N-terminal solenoid domain of Rpn6 exhibits a further conformational change to be integrated into the holocomplex by rotating around its long axis. Interestingly, a similar movement of Rpn6 was observed in the conformational change from s1 to s2/s3 state (Fig. 2). The conformational change of Rpn6 may be used to hinge the CP and the RP, and it may loosen to align the central axis of the ATPases with that of the 20S CP in the activated states.

Although a structure of the yeast 26S proteasome below 5 Å resolution was recently published (Luan et al., 2016), the structural information obtained was similar to previous reports. In contrast, two structures of the human 26S proteasome below 4 Å resolution provided further mechanical insights into the holocomplex function (Huang et al., 2016; Schweitzer et al., 2016). A surprising finding was that all six ATP binding pockets in the ATPase ring incorporate either ATP or ADP, contrary to previous assumptions of the maximum occupancy of four out of six nucleotide binding sites (Smith et al., 2011) (Fig. 3C). Intriguingly the human proteasome incorporates five ATPs and one ADP nucleotides in its ATPase ring (Schweitzer et al., 2016). Rpt6, which is located at the bottom of the 'split-washer', adopts an 'open-conformation' and binds ADP in its nucleotide binding pocket, while the other five Rpt subunits adopt a 'closed' rigid-body conformation and incorporate ATP (Schweitzer et al., 2016). The conserved two Arg residues of the arginine finger of Rpt3 point out from the ADP, while the rest of the arginine fingers are in proper placement to hold nucleotides between the small and large domains of the ATPase subunits (Fig. 3C). Further structural and biophysical studies of different conformational states are needed to elucidate the spatiotemporal dynamics of ATP binding and hydrolysis in the ATPase ring. Other prominent structural features in the human proteasome include the protrusion of the C-terminus of Rpn3 into the mouth of the ATPase ring, as well

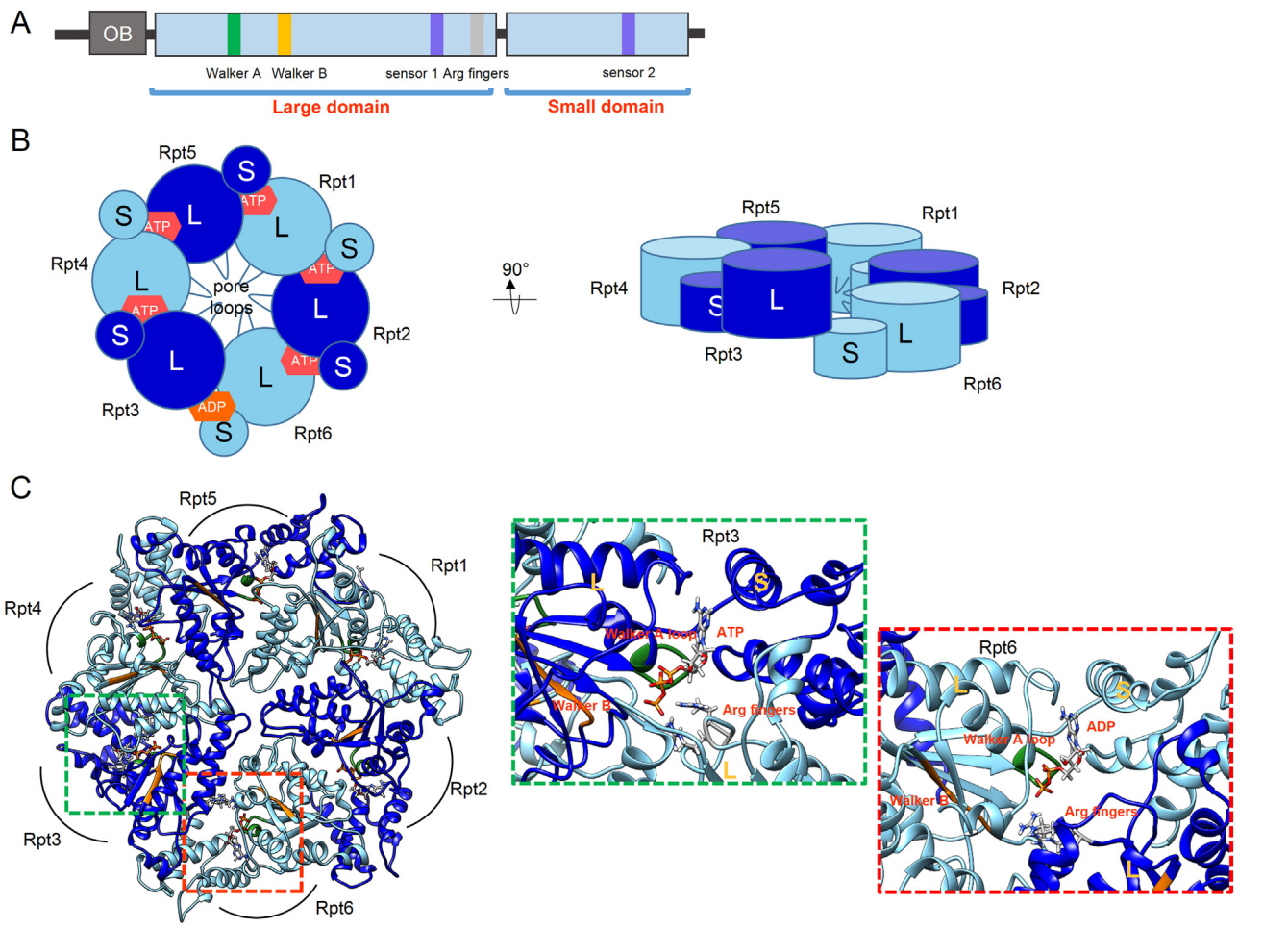

Fig. 3. (A) Domain architecture of the Rpt subunits of the human 26S proteasome (B) Schematic representation of the AAA-ATPase hexamer of the human 26S proteasome in the s1 state. Each large domain (L) of Rpt1,6,4 (light blue) and Rpt2,3,5 (blue) forms a rigid-body unit with the small domain (S) of the neighboring subunit. The nucleotide is bound within the rigid-body unit. The AAA-ATPase forms a spiral staircase interrupted between Rpt3/6. (C) Detailed view on the binding site of the nucleotides at the interface between the large and small domains of the Rpt subunits of the AAA-ATPase (pdb:5l4g). The structure of the AAA-domain of the Rpt subunits and the nucleotides are shown. The green box shows a close up view on the binding site of ATP and the red box of ADP. The walker A and B motifs are colored green and grey respectively. The arginine fingers are depicted and colored by heteroatom. All representations were made using UCSF Chimera.

as an extended connection linking two scaffold subunits Rpn1 and Rpn2 (Schweitzer et al., 2016). These linkages might be important to coordinate proteasomal subunits in a specific configuration during substrate processing.

5. Concluding remarks

Recent high-resolution structures of the 26S proteasome visualized not only some flexible and unstructured regions but also the nucleotide-binding states, which provided mechanistic insights into proteasome function. However, there are several regions which are still not resolved because of their intrinsic structural dynamics. For example, the overall structure of Rpn1 together with its associations with other subunits are poorly characterized. The N-terminal coiled coil helices of the Rpt subunits also exhibit flexibility, which might be key to substrate processing. In addition, little is known about structural basis of ubiquitylated-substrate recognition. Among four ubiquitin receptors, the EM densities of Rpn1 and the C-terminal UIM domain of Rpn10 were not well resolved because of their structural flexibility. How multiple ubiquitin receptors are utilized for substrate recognition has to be addressed in future work. Further high resolution structures of the 26S proteasome in all conformational states will allow to (1) better resolve those flexible regions and provide precise descriptions of their structure, (2) understand how ubiquitylated substrates are processed and translocated into the CP, and (3) provide further insights into the binding of polyubiquitin chains of different length and the domain movements of the AAA+ ATPase module.

Acknowledgements

We thank R. Fernandez-Busnadiego and M. R. Eisele for critical reading. This work was supported by the German Science Foundation Excellence Cluster Center for Integrated Protein Science Munich and Collaborative Research Center (SFB)-1035/Project A01 (E.S.). E. S. is supported by Marie Curie CIG (proteAmics).

References

Asano, S., Fukuda, Y., Beck, F., Aufderheide, A., Förster, F., Danev, R., Baumeister, W., 2015. A molecular census of 26S proteasomes in intact neurons. Science 347 (6220), 439–442.

Bai, X.C., Fernandez, I.S., McMullan, G., Scheres, S.H., 2013. Ribosome structures to near-atomic resolution from thirty thousand cryo-EM particles. eLife 2, e00461.

Beck, F., Unverdorben, P., Bohn, S., Schweitzer, A., Pfeifer, G., Sakata, E., Nickell, S., Plitzko, J.M., Villa, E., Baumeister, W., Forster, F., 2012. Near-atomic resolution structural model of the yeast 26S proteasome. Proc. Natl. Acad. Sci. U. S. A. 109 (37), 14870–14875.

Bohn, S., Beck, F., Sakata, E., Walzthoeni, T., Beck, M., Aebersold, R., Forster, F., Baumeister, W., Nickell, S., 2010. Structure of the 26S proteasome from

Schizosaccharomyces pombe at subnanometer resolution. Proc. Natl. Acad. Sci. U. S. A. 107 (49), 20992–20997.
Dambacher, C.M., Worden, E.J., Herzik, M.A., Martin, A., Lander, G.C., 2016. Atomic structure of the 26S proteasome lid reveals the mechanism of deubiquitinase inhibition. eLife 5, e13027.
Enemark, E.J., Joshua-Tor, L., 2006. Mechanism of DNA translocation in a replicative hexameric helicase. Nature 442 (7100), 270–275.
Erzberger, J.P., Berger, J.M., 2006. Evolutionary relationships and structural mechanisms of AAA+ proteins. Annu. Rev. Biophys. Biomol. Struct. 35, 93–114.
Estrin, E., Lopez-Blanco, J.R., Chacon, P., Martin, A., 2013. Formation of an intricate helical bundle dictates the assembly of the 26S proteasome lid. Structure 21 (9), 1624–1635.
Finley, D., 2009. Recognition and processing of ubiquitin-protein conjugates by the proteasome. Annu. Rev. Biochem 78, 477–513.
Forster, F., Lasker, K., Beck, F., Nickell, S., Sali, A., Baumeister, W., 2009. An atomic model AAA-ATPase/20S core particle sub-complex of the 26S proteasome. Biochem. Biophys. Res. Commun. 388 (2), 228–233.
Glickman, M.H., Rubin, D.M., Coux, O., Wefes, I., Pfeifer, G., Cjeka, Z., Baumeister, W., Fried, V.A., Finley, D., 1998. A subcomplex of the proteasome regulatory particle required for ubiquitin-conjugate degradation and related to the COP9-signalosome and eIF3. Cell 94 (5), 615–623.
Groll, M., Ditzel, L., Lowe, J., Stock, D., Bochtler, M., Bartunik, H.D., Huber, R., 1997. Structure of 20S proteasome from yeast at 2.4A resolution. Nature 386 (6624), 463–471.
Haglund, K., Dikic, I., 2005. Ubiquitylation and cell signaling. EMBO J. 24 (19), 3353–3359.
He, J., Kulkarni, K., da Fonseca, P.C., Krutauz, D., Glickman, M.H., Barford, D., Morris, E.P., 2012. The structure of the 26S proteasome subunit Rpn2 reveals its PC repeat domain as a closed toroid of two concentric alpha-helical rings. Structure 20 (3), 513–521.
Hershko, A., Ciechanover, A., 1998. The ubiquitin system. Annu. Rev. Biochem 67, 425–479.
Huang, X., Luan, B., Wu, J., Shi, Y., 2016. An atomic structure of the human 26S proteasome. Nat. Struct. Mol. Biol.
Kim, Y.C., Snoberger, A., Schupp, J., Smith, D.M., 2015. ATP binding to neighbouring subunits and intersubunit allosteric coupling underlie proteasomal ATPase function. Nat. Commun. 6, 8520.
Koga, N., Kameda, T., Okazaki, K., Takada, S., 2009. Paddling mechanism for the substrate translocation by AAA+ motor revealed by multiscale molecular simulations. Proc. Natl. Acad. Sci. U. S. A. 106 (43), 18237–18242.
Kuhlbrandt, W., 2014. Cryo-EM enters a new era. eLife 3, e03678.
Labbadia, J., Morimoto, R.I., 2015. The biology of proteostasis in aging and disease. Annu. Rev. Biochem 84, 435–464.
Lander, G.C., Estrin, E., Matyskiela, M.E., Bashore, C., Nogales, E., Martin, A., 2012. Complete subunit architecture of the proteasome regulatory particle. Nature 482 (7384), 186–191.
Lasker, K., Forster, F., Bohn, S., Walzthoeni, T., Villa, E., Unverdorben, P., Beck, F., Aebersold, R., Sali, A., Baumeister, W., 2012. Molecular architecture of the 26S proteasome holocomplex determined by an integrative approach. Proc. Natl. Acad. Sci. U. S. A. 109 (5), 1380–1387.
Li, X., Mooney, P., Zheng, S., Booth, C.R., Braunfeld, M.B., Gubbens, S., Agard, D.A., Cheng, Y., 2013. Electron counting and beam-induced motion correction enable near-atomic-resolution single-particle cryo-EM. Nat. Methods 10 (6), 584–590.
Lingaraju, G.M., Bunker, R.D., Cavadini, S., Hess, D., Hassiepen, U., Renatus, M., Fischer, E.S., Thoma, N.H., 2014. Crystal structure of the human COP9 signalosome. Nature.
Luan, B., Huang, X., Wu, J., Mei, Z., Wang, Y., Xue, X., Yan, C., Wang, J., Finley, D.J., Shi, Y., Wang, F., 2016. Structure of an endogenous yeast 26S proteasome reveals two major conformational states. Proc. Natl. Acad. Sci. U. S. A. 113 (10), 2642–2647.
Martin, A., Baker, T.A., Sauer, R.T., 2008. Pore loops of the AAA+ ClpX machine grip substrates to drive translocation and unfolding. Nat. Struct. Mol. Biol. 15 (11), 1147–1151.
Matyskiela, M.E., Lander, G.C., Martin, A., 2013. Conformational switching of the 26S proteasome enables substrate degradation. Nat. Struct. Mol. Biol. 20 (7), 781–788.
Nickell, S., Beck, F., Scheres, S.H., Korinek, A., Forster, F., Lasker, K., Mihalache, O., Sun, N., Nagy, I., Sali, A., Plitzko, J.M., Carazo, J.M., Mann, M., Baumeister, W., 2009. Insights into the molecular architecture of the 26S proteasome. Proc. Natl. Acad. Sci. U. S. A. 106 (29), 11943–11947.
Nogales, E., Scheres, S.H., 2015. Cryo-EM: a unique tool for the visualization of macromolecular complexity. Mol. Cell 58 (4), 677–689.
Nyquist, K., Martin, A., 2013. Marching to the beat of the ring: polypeptide translocation by AAA+ proteases. Trends Biochem. Sci.
Paraskevopoulos, K., Kriegenburg, F., Tatham Michael, H., Rösner Heike, I., Medina, B., Larsen Ida, B., Brandstrup, R., Hardwick Kevin, G., Hay Ronald, T., Kragelund Birthe, B., Hartmann-Petersen, R., Gordon, C., 2014. Dss1 is a 26S proteasome ubiquitin receptor. Mol. Cell 56 (3), 453–461.
Pathare, G.R., Nagy, I., Bohn, S., Unverdorben, P., Hubert, A., Korner, R., Nickell, S., Lasker, K., Sali, A., Tamura, T., Nishioka, T., Forster, F., Baumeister, W., Bracher, A., 2012. The proteasomal subunit Rpn6 is a molecular clamp holding the core and regulatory subcomplexes together. Proc. Natl. Acad. Sci. U. S. A. 109 (1), 149–154.
Peters, J.M., Cejka, Z., Harris, J.R., Kleinschmidt, J.A., Baumeister, W., 1993. Structural features of the 26S proteasome complex. J. Mol. Biol. 234 (4), 932–937.
Petroski, M.D., 2008. The ubiquitin system, disease, and drug discovery. BMC Biochem. 9 (Suppl. 1), S7.
Querol-Audi, J., Sun, C., Vogan, J.M., Smith, M.D., Gu, Y., Cate, J.H., Nogales, E., 2013. Architecture of human translation initiation factor 3. Structure 21 (6), 920–928.
Sakata, E., Bohn, S., Mihalache, O., Kiss, P., Beck, F., Nagy, I., Nickell, S., Tanaka, K., Saeki, Y., Forster, F., Baumeister, W., 2012. Localization of the proteasomal ubiquitin receptors Rpn10 and Rpn13 by electron cryomicroscopy. Proc. Natl. Acad. Sci. U. S. A. 109 (5), 1479–1484.
Sato, Y., Yoshikawa, A., Yamagata, A., Mimura, H., Yamashita, M., Ookata, K., Nureki, O., Iwai, K., Komada, M., Fukai, S., 2008. Structural basis for specific cleavage of Lys 63-linked polyubiquitin chains. Nature 455 (7211), 358–362.
Schwartz, A.L., Ciechanover, A., 2009. Targeting proteins for destruction by the ubiquitin system: implications for human pathobiology. Annu. Rev. Pharmacool. Toxicol. 49, 73–96.
Schweitzer, A., Aufderheide, A., Rudack, T., Beck, F., Pfeifer, G., Plitzko, J.M., Sakata, E., Schulten, K., Forster, F., Baumeister, W., 2016. Structure of the human 26S proteasome at a resolution of 3.9 A. Proc. Natl. Acad. Sci. U. S. A.
Shi, Y., Chen, X., Elsasser, S., Stocks, B.B., Tian, G., Lee, B.-H., Shi, Y., Zhang, N., de Poot, S.A.H., Tuebing, F., Sun, S., Vannoy, J., Tarasov, S.G., Engen, J.R., Finley, D., Walters, K.J., 2016. Rpn1 provides adjacent receptor sites for substrate binding and deubiquitination by the proteasome. Science 351 (6275).
Sledz, P., Unverdorben, P., Beck, F., Pfeifer, G., Schweitzer, A., Forster, F., Baumeister, W., 2013. Structure of the 26S proteasome with ATP-gammaS bound provides insights into the mechanism of nucleotide-dependent substrate translocation. Proc. Natl. Acad. Sci. U. S. A. 110 (18), 7264–7269.
Smith, D.M., Fraga, H., Reis, C., Kafri, G., Goldberg, A.L., 2011. ATP binds to proteasomal ATPases in pairs with distinct functional effects, implying an ordered reaction cycle. Cell 144 (4), 526–538.
Thomsen, N.D., Berger, J.M., 2009. Running in reverse: the structural basis for translocation polarity in hexameric helicases. Cell 139 (3), 523–534.
Thrower, J.S., Hoffman, L., Rechsteiner, M., Pickart, C.M., 2000. Recognition of the polyubiquitin proteolytic signal. EMBO J. 19 (1), 94–102.
Tomko Jr., R.J., Hochstrasser, M., 2011. Incorporation of the Rpn12 subunit couples completion of proteasome regulatory particle lid assembly to lid-base joining. Mol. Cell 44 (6), 907–917.
Tomko Jr., R.J., Funakoshi, M., Schneider, K., Wang, J., Hochstrasser, M., 2010. Heterohexameric ring arrangement of the eukaryotic proteasomal ATPases: implications for proteasome structure and assembly. Mol. Cell 38 (3), 393–403.
Tomko Jr., R.J., Taylor, D.W., Chen, Z.A., Wang, H.W., Rappsilber, J., Hochstrasser, M., 2015. A single alpha helix drives extensive remodeling of the proteasome lid and completion of regulatory particle assembly. Cell 163 (2), 432–444.
Unverdorben, P., Beck, F., Sledz, P., Schweitzer, A., Pfeifer, G., Plitzko, J.M., Baumeister, W., Forster, F., 2014. Deep classification of a large cryo-EM dataset defines the conformational landscape of the 26S proteasome. Proc. Natl. Acad. Sci. U. S. A. 111 (15), 5544–5549.
Verma, R., Aravind, L., Oania, R., McDonald, W.H., Yates 3rd, J.R., Koonin, E.V., Deshaies, R.J., 2002. Role of Rpn11 metalloprotease in deubiquitination and degradation by the 26S proteasome. Science 298 (5593), 611–615.
Voges, D., Zwickl, P., Baumeister, W., 1999. The 26S proteasome: a molecular machine designed for controlled proteolysis. Annu. Rev. Biochem. 68, 1015–1068.
Wendler, P., Ciniawsky, S., Kock, M., Kube, S., 2012. Structure and function of the AAA+ nucleotide binding pocket. Biochim. Biophys. Acta 1823 (1), 2–14.
Worden, E.J., Padovani, C., Martin, A., 2014. Structure of the Rpn11-Rpn8 dimer reveals mechanisms of substrate deubiquitination during proteasomal degradation. Nat. Struct. Mol. Biol., advance online publication.
Yao, T., Cohen, R.E., 2002. A cryptic protease couples deubiquitination and degradation by the proteasome. Nature 419 (6905), 403–407.
da Fonseca, P.C., He, J., Morris, E.P., 2012. Molecular model of the human 26S proteasome. Mol. Cell 46 (1), 54–66.